Aberrant cohesin function in *Saccharomyces cerevisiae* activates Mcd1 degradation to promote cell lethality

Running title: A cohesin surveillance mechanism

Gurvir Singh[1] and Robert V. Skibbens[1]*.

[1]Department of Biological Sciences, Lehigh University, 111 Research Drive, Bethlehem, Pennsylvania, 18015. United States of America.

* Corresponding author: Robert V. Skibbens, rvs3@lehigh.edu

Key words: Cohesins; Eco1/Ctf7/ESCO2; Rad61/WAPL; Mcd1/Scc1/RAD21; Roberts Syndrome (RBS); Cornelia de Lange Syndrome (CdLS), E3 ligase, San1, Das1, Checkpoints, sister chromatid cohesion, chromosome condensation

ABSTRACT

The cohesin complex is composed of core ring proteins (Smc1, Smc3 and Mcd1) and associated factors (Pds5, Scc3, and Rad61) that bind via Mcd1. Cohesin extrusion (looping from within a single DNA molecule) and cohesion (the tethering together of two different DNA molecules) underlie the many roles that cohesins play in chromosome segregation, gene transcription, DNA repair, chromosome condensation, replication fork progression, and genomic organization. While cohesin function flanks the activities of critical cell checkpoints (including spindle assembly and DNA damage checkpoints), the extent to which cells directly target cohesins in response to aberrant cohesin function remains unknown. Based on prior evidence that cells mutated for cohesin contain reduced Mcd1 protein, we tested whether loss of Mcd1 is based simply on cohesin instability. We find that Mcd1 loss persists even in *rad61* cells, which contain elevated levels of stable chromosome-bound cohesins, contrary to a simple instability model. In fact, re-elevating Mcd1 levels suppressed the temperature-sensitive growth defects of all cohesin alleles tested, revealing that Mcd1 loss is a fundamental mechanism through which cohesins are inactivated to promote cell lethality. Our findings further reveal that cells that exhibit aberrant cohesin function employ E3 ligases to target Mcd1 for degradation. This mechanism of degradation appears unique in that Mcd1 is reduced during S phase, when Mcd1 levels typically peak and despite a dramatic upregulation in *MCD1* transcription. We infer from these latter findings that cells contain a negative feedback mechanism used to maintain Mcd1 homeostasis.

AUTHOR SUMMARY

Cohesins are central to almost all aspects of DNA regulation (chromosome segregation, gene transcription, DNA repair, chromosome condensation, replication fork progression, and genomic organization). Cohesin also play key roles in cell checkpoints: cohesin mutations activate the spindle assembly checkpoint while double strand DNA breaks can elicit a new round of cohesin establishment. In the current study, we provide evidence for a novel cohesin surveillance system that employs E3 ligases that directly target Mcd1, a core component of the cohesin ring structure, for degradation during S phase. We further describe a feedback mechanism through which cells dramatically induce *MCD1* transcription to maintain Mcd1 homeostasis. Finally, we provide evidence that requires the re-evaluation of phenotypes associated with other cohesin gene mutations.

INTRODUCTION

The identification of checkpoints has produced significant clinical advances over the last half century (1, 2). After the discovery that the tumor suppressor p53 is mutated in more than 50% of all cancers, advances from both basic science and clinical settings led to new strategies through which p53 can be re-activated, mutated p53 degraded, or synthetic lethal mechanisms to eliminate cancer cells (3–7). Similarly, highly proliferative cancer cells are disproportionally sensitive to spindle assembly checkpoint inhibitors, compared to non-tumorigenic cells (8–10). Often, factors that exhibit multiple functions, or reside at the nexus of critical pathways, are monitored by surveillance mechanisms and provide important avenues to improve human health.

Cohesins are ATPase protein complexes composed of a core ring (Smc1, Smc3 and Mcd1) and associated factors (Pds5, Scc3, and Rad61) that bind via Mcd1. Cohesins are central to almost all aspects of DNA regulation (chromosome segregation, gene transcription, DNA repair, chromosome condensation, replication fork progression, and genomic organization)(11–28). Underlying this complex output of roles, cohesins perform two essential functions: extrusion (looping from within a single DNA molecule) and cohesion (the tethering together of two different DNA molecules) (11, 12, 16, 17, 21–23). Mutations in cohesins that affect DNA looping can give rise to severe developmental abnormalities such as Cornelia De Lange Syndrome (CdLS) and Roberts Syndrome (RBS). These multifaceted maladies often include intellectual disabilities, hearing loss, microcephaly, phocomelia and abnormalities in the heart and gastrointestinal tract (29–35). Mutations that impact tethering give rise to aneuploidy - a

hallmark of cancer cells(36–38). Recent evidence indeed suggests that cancer cells rely on elevated cohesin activity for survival (39–43).

It is well established that cohesin functions flank critical cell checkpoints. For instance, cohesin mutations that abolish sister chromatid cohesion (tethering) activate the spindle assembly checkpoint (44–46), consistent with classic micromanipulation and laser ablation studies that cells monitor chromosome biorientation, and thus tension, produced across the two mitotic half-spindles (47–52). In contrast, double strand DNA breaks activate ATM/ATR and CHK1 kinases that elicit a *de novo* round of cohesin deposition and cohesion establishment both at sites of damage and genome-wide (13, 19, 53–59). The remarkable involvement of cohesins in cell cycle checkpoints, both to maintain euploidy and promote error-free DNA damage repair, underscores their central role in maintaining genome integrity.

In this study, we present evidence that cohesins are a direct target of a surveillance system that may cull aneuploid or transcriptionally aberrant cells from a normal population. The current study was motivated, in part, by previously unexplained observations that cohesin mutations result in a significant reduction of Mcd1 protein (60–63). Rad61 (or the human homolog WAPL) promotes cohesin dissociation from DNA, such that cells with reduced Rad61/WAPL activity contain elevated levels of stable chromosome-bound cohesins, prematurely condensed (and even hyper-condensed) chromatin (64–69). Despite this hyperstabilization of cohesin complexes, our results reveal that Mcd1 is significantly reduced in *rad61* deleted cells. The reduction of Mcd1 in the absence of a temperature-sensitive cohesin allele, and during S phase when Mcd1 levels typically peak, argue against a simple model that cohesin

instability accounts for Mcd1 loss. Intriguingly, *MCD1* transcription is dramatically upregulated during S phase despite the reduction in Mcd1 protein levels, suggesting that a novel feedback mechanism typically is in place to maintain Mcd1 homeostasis.

RESULTS

Rad61 positively regulates cohesins through Mcd1

The majority of cohesin-mutated cells tested to date (*smc1-259*, *smc3-42*, *pds5-1*, *pds5Δ elg1Δ*, and *eco1Δ rad61Δ*) contain significantly reduced levels of Mcd1 protein (60–63). Rad61 dissociates cohesin from DNA such that *rad61Δ* cells retain elevated levels of stably-bound cohesins (65–73). Given the opposing activities of Eco1 (cohesin stabilization) and Rad61 (cohesin dissociation), we hypothesized that *rad61Δ* cells should retain wildtype levels of Mcd1 and suppress the loss of Mcd1 in *eco1* mutated cells. To test these predictions, log phase cultures of wildtype, *rad61Δ*, *eco1-203*, and *eco1Δ rad61Δ* cells were arrested in early S phase (hydroxyurea, HU) prior to shifting to 37°C (Figure 1A). Surprisingly, Western blot quantifications of the resulting mitotic extracts revealed that Mcd1 levels are reduced not only in *eco1* temperature-sensitive (ts) strains, but also significantly reduced in *rad61Δ* cells (Figures 1B, 1C). Nor did the deletion of *RAD61* provide any benefit to *eco1Δ* cells with respect to Mcd1 levels (Figures 1B, 1C). These results suggest that Mcd1 levels may be reduced by a surveillance system that monitors for aberrant cohesin function beyond cohesin complex stability.

A negative feedback loop regulates *MCD1* expression

The near ubiquitous reduction of Mcd1 in cohesin-mutated cells prompted us to uncover the underlying molecular mechanism. Mcd1 is unique among cohesin subunits in that it is the only core subunit that is degraded at anaphase onset (to allow for sister chromatid segregation), and then transcribed starting at the G1/S transition, each and every cell cycle (11, 62, 74). Previous findings documented a complex transcriptional network that regulates *MCD1* expression (61). It thus became important to test the extent to which *MCD1* transcription is reduced in the *eco1Δ rad61Δ* cells. Log phase wildtype and *eco1Δ rad61Δ* cells were arrested in early S phase (HU, hydroxyurea) (Figure 2A) - a point in the cell cycle at which *MCD1* expression and Mcd1 protein levels peak in wildtype cells, but in which Mcd1 protein levels are significantly reduced in *eco1Δ rad61Δ* cells (11, 61). We confirmed that Mcd1 protein levels were significantly reduced in the same *eco1 rad61* cultures (Figures 2B, 2C) used to test for changes in *MCD1* transcription. In contrast to the model that *MCD1* transcription is decreased, quantification of qRT-PCR revealed that *MCD1* transcript levels are instead significantly increased (~5.5 fold) in *eco1Δ rad61Δ* cells compared to wildtype cells (Figure 2D). These results indicate that the loss of Mcd1 protein in *eco1Δ rad61Δ* cells is not dependent on reduced *MCD1* transcription. Moreover, our findings reveal a compensatory feedback mechanism in which cells increase *MCD1* transcription in response to decreased Mcd1 protein levels.

An E3 ligase mechanism promotes Mcd1 degradation

Having excluded a transcription-based mechanism, it became important to test the extent to which the reduction in Mcd1 protein level occurs through degradation. Mcd1 is reduced in early S phase in *eco1Δ rad61Δ* cells, suggesting that a degradation mechanism is likely independent of Esp1, a caspase-type protease that cleaves Mcd1 during anaphase onset (61, 74–76). To formally test this hypothesis, *eco1Δ rad61Δ* cells and *esp1-1* cells were mated and the resulting diploids sporulated and dissected. Reduced Esp1 activity, however, failed to suppress *eco1Δ rad61Δ* cells ts growth defects (data not shown), consistent with a role for Esp1 that is predominantly limited to mitosis (74, 76).

Protein ubiquitination, through E3 ligases, play key roles in numerous cellular activities that include degradation (77, 78). Thus, we focused on E3 ligases as a mechanism required to reduce Mcd1 protein levels, a model supported by prior evidence that Mcd1 is a target of ubiquitination (79, 80). The E3 ligases that target Mcd1 remained unidentified, requiring us to generate a candidate list based on genetic or physical interactions (BioGrid and SGD) across various cohesins subunits (81–84). We prioritized our efforts on five candidates (Bre1, Bul2, Lbd19, Das1, and San1), all of which are encoded by non-essential genes. We reasoned that if any of the candidates E3 ligases are in part responsible for ubiquitinating Mcd1, then their deletion should suppress *eco1Δ rad61Δ* cell ts growth defects. To test this model, each of the E3 ligases genes (*BRE1*, *BUL2*, *LBD19*, *DAS1* and *SAN1*) were individually deleted from wildtype and *eco1Δ rad61Δ* cells. Log phase cultures of the resulting transformants were serially diluted onto rich medium plates and incubated at either 30°C or 37°C, temperatures respectively permissive and non-permissive for *eco1Δ rad61Δ* cell growth (Figure 3).

Deletion of *BUL2* had no impact on either wildtype or *eco1Δ rad61Δ* cells at either temperature (Figure 3A). Deletion of *BRE1* exhibited an adverse effect on both wildtype and *eco1Δ rad61Δ* cells (Figure 3B), consistent with a prior report that *bre1Δ* cells exhibit genomic instability (85). Compared to the adverse but non-specific impact of *BRE1* deletion, deletion of *LBD19* produced a severe negative impact specific to *eco1Δ rad61Δ* cells (Figure 3C). In contrast to the results above, deletion of *SAN1*, and to a lesser extent *DAS1*, suppressed the ts growth defects otherwise exhibited by *eco1Δ rad61Δ* cells (Figure 3D, 3E). Thus, E3 ligases San1 and Das1 play critical roles in Mcd1 degradation in response to reduced cohesin function.

MCD1 overexpression rescues the inviabilty of cohesin mutated cells

The reduction in Mcd1 protein levels is an attribute common to all cohesin-mutated cells tested to date (60–63, this study). This near ubiquitous reduction in Mcd1 prompted us to ask the following question: are cohesin mutated cell ts-lethalities due to the mutated cohesin allele (ie. Mcd1 loss is a downstream consequence of cohesin inactivation, but otherwise unimportant) or due to the reduction in Mcd1? To differentiate between these two possibilities, we tested the extent to which elevated expression of *MCD1* could suppress the lethality of cells that harbor ts mutations in other cohesin genes. Wildtype, *eco1-1*, *scc3-6*, *smc3-42*, and *smc1-259* cells were each transformed with either vector alone or vector driving elevated expression of *MCD1* and log phase culture of the resulting transformants serially diluted onto selective media plates. As expected, elevated *MCD1* expression had no effect on the growth of wildtype cells at the temperatures tested. In contrast, overexpression of *MCD1* suppressed the ts

growth defects in all five cohesin ts alleles (Figure 4) - in some cases up to the elevated temperature of 37°C. We further found that elevated *MCD1* expression suppressed the ts growth defect of *scc2-4* mutant cells in which mutation of a cohesin subunits is fully absent (Figure 4E). These results not only provide evidence that loss of Mcd1 significantly contributes to the lethality of cohesin-mutated cells, but also confound prior interpretations of the severity of phenotypes attributed solely to those ts alleles.

Mcd1 differentially contributes to cohesion and condensation

Above, we established Mcd1 as a key driver of most, if not all, cohesin-mutated strain lethalities. It next became important to test which if any cohesin functions are rescued by elevated Mcd1 levels in cells that harbor mutation in another cohesin gene. Wildtype and *smc1-259* strains were genetically modified to contain either an rDNA condensation marker (Net1-GFP) or a cohesion assay cassette (tetO and TetR-GFP) (11, 12, 20, 69, 72, 86, 87). The modified strains were then transformed with a high-copy vector alone or vector that drives elevated expression of *MCD1*. Log phase cultures of the resulting transformants were arrested in G1 (alpha factor, αF) and then released into 34°C (non-permissive for *smc1-259* cells) rich medium that contains nocodazole (NZ) to arrest cells in preanaphase. DNA content (flow cytometry) and cell morphologies were monitored at various stages of both experiments (Figures 5A, 6A).

Notably, *smc1-259* mutant cells have not been previously assessed for condensation defects. Here, we exploited the well-established analysis of rDNA chromatin architecture using Ne1-GFP (11, 20, 69, 72, 88). In wildtype cells, rDNA converts from a decondensed puff-like structure during G1 into tight loops (occasionally

observed as bars) during mitosis (89). As expected, wildtype cells arrested in preanaphase exhibited well-defined rDNA loops, indicative of robust chromosome condensation (Figure 5B, 5C). In contrast, only 21% of *smc1-259* cells contained tight loops such that the majority of cells exhibited defects in rDNA condensation (Figure 5B, 5C). These results extend prior findings regarding the condensation defects exhibited by other cohesin mutated strains (11, 28, 44, 71, 90–92). Elevated expression of *MCD1* had no observable impact on rDNA structure in wildtype cells. Surprisingly, *MCD1* expression produced only a modest increase (38%, compared to 21% in the vector control) in the percent of *smc1-259* cells that contained condensed rDNA loops (Figure 5C). Given prior evidence that suppression of condensation defects underlies the improved viability of cohesin-mutated cells (93), we decided to further investigate the condensation of rDNA structure. Mutated cells that did not contain tight and well-defined rDNA loops were parsed into two categories: puff-like (fully decondensed) and in which some structure was apparent within the rDNA mass (partial decondensation). Focusing on the more severe of the two phenotypes, *smc1-259* cells that contained vector alone were strongly biased toward the frequency of puffs (~65% puffs compared to 12% partial condensed) (Figure 5D). *smc1-259* cells in which *MCD1* was over expressed, however, contained a significant decrease in the frequency of puffs (25%, down from 65% for vector alone) (Fig 5D). In combination, these findings reveal that Mcd1 exerts a relatively limited impact on rDNA condensation.

Next, we assessed the effect of elevated *MCD1* expression on sister chromatid cohesion. In wildtype cells, the GFP-marked tetO that marks each sister chromatid are closely tethered together to appear as a single dot. In cohesin mutated cells, the

separated sisters are readily detected as two dots (12). Elevated expression of *MCD1* had no effect on sister chromatid cohesion such that wildtype cells contained very high frequencies of tethered sister chromatids (1 dot/nucleus), regardless of harboring vector alone or vector expressing *MCD1* (Figure 6). *smc1-259* cells that contained vector alone exhibited a high (60%) frequency of 2 dots/nucleus (Figure 6), consistent with prior studies and the frequency of cohesion defects observed in other cohesin mutated cells (11, 44, 90, 91, 93, 94). Notably, elevated expression of *MCD1* significantly restored sister chromatid tethering in *smc1-259* cells, with only 35% (compared to 60% vector control) of cells exhibiting cohesion defects. Thus, elevated *MCD1* expression is sufficient to elicit a robust rescue in cohesion, but not condensation, defects. More importantly, cell defects in condensation, compared to cohesion, appear largely attributable to the *smc1-259* allele.

DISCUSSION

The core cohesin component, Mcd1, which caps the ATPase domains of Smc1 and Smc3 in core cohesin complexes, is greatly reduced in cells that harbor mutations in nearly every cohesin gene tested to date (60–63, this study). A priori, a simple explanation is that cohesin gene mutations destabilize the cohesin ring and, in some fashion, promote the loss of the non-mutated Mcd1 protein. The first revelation of the current study is that Mcd1 is significantly reduced in *rad61Δ* strains - cells in which cohesins appear hyper-stabilized, exhibit extended DNA-association and exhibit increased cohesin activities that include chromosome compaction and DNA loop formation (61, 65–69, 71–73, 95, 95). Moreover, Mcd1 is reduced in the absence of

elevated temperatures (*eco1 rad61*), in the absence of a ts cohesin allele (*rad61*), and re-elevating Mcd1 levels suppresses the ts growth defects of cells that harbor no cohesin subunit allele (*scc2-4*). These findings, coupled with the recognition that it is wildtype Mcd1 protein that is reduced, rather than a mutated or misfolded version, are inconsistent with a simple instability model.

What signals Mcd1 degradation? It is tempting to speculate that cells respond to defective or aberrant cohesin functions by activating a unique mechanism to cull out cells that might otherwise contribute to an aneuploid or developmentally-altered population. Mcd1 targeting may not be exclusive to cells that incur cohesin defects given that exposure to reactive oxygen species also triggers Mcd1 degradation in an apoptotic response that includes the caspase-like Esp1 (96–99). The conserved nature of this targeting mechanism is further supported by findings that RAD21 (homolog of Mcd1) is degraded by caspases 3 and 7 during apoptotic responses (96, 100, 101). Together, these results suggest that inactivating cohesin functions through Mcd1 degradation may represent an evolutionarily conserved mechanism for promoting cell death.

The second set of findings that emerge from the current study is the identification of the pathway through which Mcd1 is degraded. In unperturbed cells, Mcd1 is degraded at anaphase onset by Esp1. Here, our findings largely negate a role for an Esp1-dependent mechanism during S phase and instead document novel roles for E3 ligases (San1 and Das1) in promoting Mcd1 degradation during S phase, a time when Mcd1 levels typically peak. How information that arises from cohesin defects might be relayed to E3 ligases remains unknown. Recent evidence, however, suggests that the Cln2-

containing G1 CDK plays a critical role. For instance, deletion of *CLN2* rescues both *eco1 rad61* cell ts growth defects and *pds5 elg1* lethality - both through increased Mcd1 levels (60, 68). These findings support a mechanism in which cohesin defects (or aberrant functioning) from the prior cell cycle activate Cln2-CDK to promote E3 ligase-dependent degradation of Mcd1. It will be important to test whether these preceding defects might include retention of an activated spindle checkpoint (due to cohesion defects) or transcriptional abnormalities that arise due to defects in cohesin extrusion activities.

The findings reported here impact all prior analyses of cohesin mutated strains. The lethality of mutated cohesin strains alleles were interpreted to reflect protein inactivation/misfolding of the mutated protein. Instead, we find substantial suppression of the ts growth defects that occur in cohesin mutated cells (*smc1*, *smc3*, *scc3*, *scc2* and *eco1*) simply by re-elevating Mcd1 levels. Previously, the severity of cohesin phenotypes (loss of sister chromatid cohesion, defects in chromosome condensation, and genotoxic sensitivities) were found to scale closely to changes in Mcd1 levels (102). We were thus intrigued by the possibility that elevated *MCD1* might differentially suppress phenotypes otherwise exhibited by cohesin mutated strains. Indeed, our findings reveal that re-elevating Mcd1 produces a more robust rescue of cohesion defects, compared to the rescue of condensation defects in *smc1-259* cells. We infer from these findings that Mcd1-dependent restoration of cohesion primarily accounts for the decrease in temperature-sensitive growth of *smc1-259* cells. These results further reveal that Smc1 appears to have a greater role in condensation, compared to cohesion, than previously reported. In combination, these findings suggest that a re-

evaluation regarding the severity of associated alleles is warranted. More broadly, studies that characterize phenotypes for a mutated component within a complex should be coupled with analyses regarding the persistence of the remaining subunits.

The final revelation of the current study relates to the mechanism through which yeast cells achieve homeostatic levels of Mcd1. Subsequent to degradation at anaphase onset, Mcd1 levels rise starting at the G1/S transition and peak during S phase. Our results suggest that Mcd1 protein negatively regulates its own expression such that E3-ligase degradation Mcd1 results in a dramatic upregulation in *MCD1* expression during S phase. Notably, the balance heavily favors degradation over transcription, suggesting that E3 ligases become significantly activated (compared to the approximately 5.5-fold increase in *MCD1* transcription) in response to cohesin defects.

MATERIALS AND METHODS

Yeast strains, media, and growth conditions: All strains (see Supplementary Table 1 for strain genotypes) were grown on YPD-rich media unless placed on selective medium to facilitate plasmid transformation/retention or spore identification (103).

Strain generation: Primers used to delete genes (*BUL2*, *BRE1*, *LBD19*, *DAS1* and *SAN1*) and verify proper integration are listed in Supplementary Table 2. GFP-tagging Net1, to include either *kanMX6* or *TRP1* markers, are previously described (104). The cohesion assay strains used in this study (YGS333, YGS334, YGS321, YGS323) were generated by crossing *smc1-259* (YBS3168/ K6013) with wildtype cells that harbor the cohesion assay cassette (*tetO:URA3 tetR-GFP:LEU2 Pds1-Myc:TRP1*)

(YBS1042) (87, 105). The resulting diploid (YGS301) was sporulated and dissected to obtain *smc1-259 tetO:URA3 tetR-GFP:LEU2* cells and wildtype cassette strain *tetO:URA3 tetR-GFP:LEU2*.

Wildtype and cohesin mutant cells overexpressing vector were transformed with either pRS424 plasmid (2μ *TRP1*) or pRS425 (2μ *LEU*) and cells overexpressing *MCD1* were transformed either with pRS425 (2μ *LEU*) or pGS35 (2μ *LEU2 MCD1*) (61). See Supplementary Table 1 for resulting strain names and genotypes.

Western Blots: Cell numbers for each log phase strain were normalized to 2 OD_{600}. Whole cell protein extracts were prepared as described in (106) with minor modifications. Cells were mechanically lysed (Bead-beater, BioSpec) in 17% TCA with regular intermittent cooling on ice. The beads were washed two times in 500μL of 5% TCA and the two lysates combined and centrifuged at 15,000 rpm for 20 min at 4°C with subsequent solubilization in 3% SDS and 0.25 M Tris-base buffer. Western blotting and protein detection using the anti-Mcd1 antibody (generous gift from Dr. Vincent Guacci), anti-PGK1 (Invitrogen), Goat anti-Mouse HRP (BIO-RAD) or Goat anti-Rabbit HRP (BIO-RAD), were performed as previously described (61). Protein band intensities (obtained by ChemiDoc™ MP) were quantified using Image J. Significance was determined by a two-tailed test as described in legends.

RNA extraction and qRT-PCR: Cell numbers from log phase cultures were normalized to 2 OD_{600} , pelleted by centrifugation and frozen in liquid nitrogen. Cells were lysed mechanically using a bead-beater (BioSpec) for 8 min with intermittent cooling on ice. RNA was extracted and purified using the RNeasy Mini Kit (Qiagen) per manufacturer's instructions and quantified using a nanodrop (Thermo Scientific,

NanoDrop One^{C}). Normalized RNAs were treated with Turbo DNase (Ambion) and then reverse transcribed using SupercriptIII (Invitrogen). Quantitative Real -Time (qRT) PCR was performed in triplicates using the Rotor-Gene SYBR Green PCR kit (Cat. No. 204074) and C_T values measured using the Rotor Gene (Corbett). C_T values of *MCD1* and internal control ALG9 were averaged and the fold change in *MCD1* expression determined using the $2^{-\Delta\Delta Ct}$method (107).

Condensation and Cohesion Assays: Cohesion and condensation assays were performed as previously described (86) with the following modifications. Log phase cells were grown in selective media, followed by pre-synchronized in G1 (alpha factor) for 3 hr at 23°C in YPD- rich media. The resulting cultures were harvested, washed 2 times and then shifted to 37°C for 3 hr in fresh media supplemented with nocodazole. Cell aliquots of the resulting preanaphase arrested cells were fixed at room temperature in paraformaldehyde to a final concentration of 3.7%. Cells were assayed using an E800 light microscope (Nikon) equipped with a cooled CD camera (Coolsnapfx, Photometrics) and imaging software (IPLab, Scanalytics).

Flow Cytometry and Cell Cycle Progression: Log phase cultures were normalized (OD_{600}) and synchronized at specific cell stages using the following treatments: early S phase with 0.2 M Hydroxyurea (SIGMA, H8627), G1 phase with 3 µM alpha factor (ZYMO RESEARCH, Y1001), M phase with 20 µg/ml of nocodazole (SIGMA, M1404). Log phase growth and proper cell cycle arrest were confirmed by flow cytometry as previously described (86, 95).

ACKNOWLEDGEMENTS

The authors gratefully acknowledge the generous gifts of Mcd1-directed antibody and numerous yeast strains from Dr. Vincent Guacci and the Koshland Lab. The authors also Skibbens lab members and participants in the Super Group Yeast Club for helpful discussions during the preparation of this paper.

REFERENCES

1. L. H. Hartwell, T. A. Weinert, Checkpoints: Controls That Ensure the Order of Cell Cycle Events. *Science* **246**, 629–634 (1989).
2. R. Uzbekov, C. Prigent, A Journey through Time on the Discovery of Cell Cycle Regulation. *Cells* **11**, 704 (2022).
3. M. Masutani, T. Nozaki, K. Wakabayashi, T. Sugimura, Role of poly(ADP-ribose) polymerase in cell-cycle checkpoint mechanisms following γ-irradiation. *Biochimie* **77**, 462–465 (1995).
4. S. Tsukamoto, Natural products that target p53 for cancer therapy. *J Nat Med* **79**, 725–737 (2025).
5. S. Nishikawa, T. Iwakuma, Drugs Targeting p53 Mutations with FDA Approval and in Clinical Trials. *Cancers* **15**, 429 (2023).
6. W. Li, F. Wang, R. Guo, Z. Bian, Y. Song, Targeting macrophages in hematological malignancies: recent advances and future directions. *J Hematol Oncol* **15** (2022).
7. P. Baliakas, T. Soussi, The TP53 tumor suppressor gene: From molecular biology to clinical investigations. *J Intern Med* **298**, 78–96 (2025).

8. B. A. A. Weaver, D. W. Cleveland, Decoding the links between mitosis, cancer, and chemotherapy: The mitotic checkpoint, adaptation, and cell death. *Cancer Cell* **8**, 7–12 (2005).

9. K. Tanaka, T. Hirota, Chromosome segregation machinery and cancer. *Cancer Science* **100**, 1158–1165 (2009).

10. J. Gallego-Jara, G. Lozano-Terol, R. A. Sola-Martínez, M. Cánovas-Díaz, T. De Diego Puente, A Compressive Review about Taxol®: History and Future Challenges. *Molecules* **25**, 5986 (2020).

11. V. Guacci, D. Koshland, A. Strunnikov, A Direct Link between Sister Chromatid Cohesion and Chromosome Condensation Revealed through the Analysis of MCD1 in S. cerevisiae. *Cell* **91**, 47–57 (1997).

12. C. Michaelis, R. Ciosk, K. Nasmyth, Cohesins: Chromosomal Proteins that Prevent Premature Separation of Sister Chromatids. *Cell* **91**, 35–45 (1997).

13. C. Sjögren, K. Nasmyth, Sister chromatid cohesion is required for postreplicative double-strand break repair in Saccharomyces cerevisiae. *Current Biology* **11**, 991–995 (2001).

14. R. Jessberger, The many functions of smc proteins in chromosome dynamics. *Nat Rev Mol Cell Biol* **3**, 767–778 (2002).

15. J.-S. Kim, T. B. Krasieva, V. LaMorte, A. M. R. Taylor, K. Yokomori, Specific Recruitment of Human Cohesin to Laser-induced DNA Damage. *Journal of Biological Chemistry* **277**, 45149–45153 (2002).

16. E. de Wit, *et al.*, CTCF Binding Polarity Determines Chromatin Looping. *Molecular Cell* **60**, 676–684 (2015).

17. I. F. Davidson, *et al.*, Rapid movement and transcriptional re-localization of human cohesin on DNA. *The EMBO Journal* **35**, 2671–2685 (2016).
18. M.-E. Terret, R. Sherwood, S. Rahman, J. Qin, P. V. Jallepalli, Cohesin acetylation speeds the replication fork. *Nature* **462**, 231–234 (2009).
19. E. Ünal, J. M. Heidinger-Pauli, D. Koshland, DNA Double-Strand Breaks Trigger Genome-Wide Sister-Chromatid Cohesion Through Eco1 (Ctf7). *Science* **317**, 245–248 (2007).
20. T. Hartman, K. Stead, D. Koshland, V. Guacci, Pds5p Is an Essential Chromosomal Protein Required for Both Sister Chromatid Cohesion and Condensation in *Saccharomyces cerevisiae*. *The Journal of Cell Biology* **151**, 613–626 (2000).
21. J. H. I. Haarhuis, *et al.*, The Cohesin Release Factor WAPL Restricts Chromatin Loop Extension. *Cell* **169**, 693-707.e14 (2017).
22. S. S. P. Rao, *et al.*, Cohesin Loss Eliminates All Loop Domains. *Cell* **171**, 305-320.e24 (2017).
23. G. Wutz, *et al.*, Topologically associating domains and chromatin loops depend on cohesin and are regulated by CTCF, WAPL, and PDS5 proteins. *The EMBO Journal* **36**, 3573–3599 (2017).
24. E. Lara-Pezzi, *et al.*, Evidence of a Transcriptional Co-activator Function of Cohesin STAG/SA/Scc3. *Journal of Biological Chemistry* **279**, 6553–6559 (2004).
25. R. A. Rollins, P. Morcillo, D. Dorsett, Nipped-B, a Drosophila Homologue of Chromosomal Adherins, Participates in Activation by Remote Enhancers in the cut and Ultrabithorax Genes. *Genetics* **152**, 577–593 (1999).

26. R. A. Rollins, M. Korom, N. Aulner, A. Martens, D. Dorsett, *Drosophila* Nipped-B Protein Supports Sister Chromatid Cohesion and Opposes the Stromalin/Scc3 Cohesion Factor To Facilitate Long-Range Activation of the *cut* Gene. *Molecular and Cellular Biology* **24**, 3100–3111 (2004).

27. R. V. Skibbens, J. Marzillier, L. Eastman, Cohesins coordinate gene transcriptions of related function within*Saccharomyces cerevisiae*. *Cell Cycle* **9**, 1601–1606 (2010).

28. S. Gard, *et al.*, Cohesinopathy mutations disrupt the subnuclear organization of chromatin. *Journal of Cell Biology* **187**, 455–462 (2009).

29. I. D. Krantz, *et al.*, Cornelia de Lange syndrome is caused by mutations in NIPBL, the human homolog of Drosophila melanogaster Nipped-B. *Nat Genet* **36**, 631–635 (2004).

30. E. T. Tonkin, T.-J. Wang, S. Lisgo, M. J. Bamshad, T. Strachan, NIPBL, encoding a homolog of fungal Scc2-type sister chromatid cohesion proteins and fly Nipped-B, is mutated in Cornelia de Lange syndrome. *Nat Genet* **36**, 636–641 (2004).

31. B. Schüle, A. Oviedo, K. Johnston, S. Pai, U. Francke, Inactivating Mutations in ESCO2 Cause SC Phocomelia and Roberts Syndrome: No Phenotype-Genotype Correlation. *The American Journal of Human Genetics* **77**, 1117–1128 (2005).

32. H. Vega, *et al.*, Roberts syndrome is caused by mutations in ESCO2, a human homolog of yeast ECO1 that is essential for the establishment of sister chromatid cohesion. *Nat Genet* **37**, 468–470 (2005).

33. A. Musio, *et al.*, X-linked Cornelia de Lange syndrome owing to SMC1L1 mutations. *Nat Genet* **38**, 528–530 (2006).

34. M. A. Deardorff, *et al.*, Mutations in Cohesin Complex Members SMC3 and SMC1A Cause a Mild Variant of Cornelia de Lange Syndrome with Predominant Mental Retardation. *The American Journal of Human Genetics* **80**, 485–494 (2007).

35. M. Gordillo, *et al.*, The molecular mechanism underlying Roberts syndrome involves loss of ESCO2 acetyltransferase activity. *Human Molecular Genetics* **17**, 2172–2180 (2008).

36. J. Antony, C. V. Chin, J. A. Horsfield, Cohesin Mutations in Cancer: Emerging Therapeutic Targets. *Int J Mol Sci* **22**, 6788 (2021).

37. M. Di Nardo, M. M. Pallotta, A. Musio, The multifaceted roles of cohesin in cancer. *J Exp Clin Cancer Res* **41**, 96 (2022).

38. D. Pati, Role of chromosomal cohesion and separation in aneuploidy and tumorigenesis. *Cell Mol Life Sci* **81**, 100 (2024).

39. J. Yun, *et al.*, Reduced cohesin destabilizes high-level gene amplification by disrupting pre-replication complex bindings in human cancers with chromosomal instability. *Nucleic Acids Res* **44**, 558–572 (2016).

40. H. Xu, *et al.*, Enhanced RAD21 cohesin expression confers poor prognosis and resistance to chemotherapy in high grade luminal, basal and HER2 breast cancers. *Breast Cancer Res* **13** (2011).

41. P. Sarogni, *et al.*, Overexpression of the cohesin-core subunit SMC1A contributes to colorectal cancer development. *J Exp Clin Cancer Res* **38** (2019).

42. Y. Huang, *et al.*, ESCO2's oncogenic role in human tumors: a pan-cancer analysis and experimental validation. *BMC Cancer* **24** (2024).

43. W. Gan, *et al.*, Prognostic Values and Underlying Regulatory Network of Cohesin Subunits in Esophageal Carcinoma. *J Cancer* **13**, 1588–1602 (2022).

44. R. V. Skibbens, L. B. Corson, D. Koshland, P. Hieter, Ctf7p is essential for sister chromatid cohesion and links mitotic chromosome structure to the DNA replication machinery. *Genes & Development* **13**, 307–319 (1999).

45. K. Tanaka, *et al.*, Fission Yeast Eso1p Is Required for Establishing Sister Chromatid Cohesion during S Phase. *Molecular and Cellular Biology* **20**, 3459–3469 (2000).

46. Md. T. Hoque, F. Ishikawa, Cohesin Defects Lead to Premature Sister Chromatid Separation, Kinetochore Dysfunction, and Spindle-assembly Checkpoint Activation. *Journal of Biological Chemistry* **277**, 42306–42314 (2002).

47. X. Li, R. B. Nicklas, Mitotic forces control a cell-cycle checkpoint. *Nature* **373**, 630–632 (1995).

48. R. B. Nicklas, How Cells Get the Right Chromosomes. *Science* **275**, 632–637 (1997).

49. J. Kuhn, S. Dumont, Mammalian kinetochores count attached microtubules in a sensitive and switch-like manner. *Journal of Cell Biology* **218**, 3583–3596 (2019).

50. J. R. Aist, H. Liang, M. W. Berns, Astral and spindle forces in PtK2 cells during anaphase B: a laser microbeam study. *Journal of Cell Science* **104**, 1207–1216 (1993).

51. C. L. Rieder, E. A. Davison, L. C. Jensen, L. Cassimeris, E. D. Salmon, Oscillatory movements of monooriented chromosomes and their position relative to the spindle

pole result from the ejection properties of the aster and half-spindle. *The Journal of cell biology* **103**, 581–591 (1986).

52. R. V. Skibbens, C. L. Rieder, E. D. Salmon, Kinetochore motility after severing between sister centromeres using laser microsurgery: Evidence that kinetochore directional instability and position is regulated by tension. *Journal of Cell Science* **108**, 2537–2548 (1995).
53. S.-T. Kim, B. Xu, M. B. Kastan, Involvement of the cohesin protein, Smc1, in Atm-dependent and independent responses to DNA damage. *Genes Dev* **16**, 560–570 (2002).
54. E. Ünal, *et al.*, DNA Damage Response Pathway Uses Histone Modification to Assemble a Double-Strand Break-Specific Cohesin Domain. *Molecular Cell* **16**, 991–1002 (2004).
55. L. Ström, H. B. Lindroos, K. Shirahige, C. Sjögren, Postreplicative Recruitment of Cohesin to Double-Strand Breaks Is Required for DNA Repair. *Molecular Cell* **16**, 1003–1015 (2004).
56. L. Ström, *et al.*, Postreplicative Formation of Cohesion Is Required for Repair and Induced by a Single DNA Break. *Science* **317**, 242–245 (2007).
57. X. Kong, *et al.*, Distinct Functions of Human Cohesin-SA1 and Cohesin-SA2 in Double-Strand Break Repair. *Molecular and Cellular Biology* **34**, 685–698 (2014).
58. H. Luo, *et al.*, Regulation of Intra-S Phase Checkpoint by Ionizing Radiation (IR)-dependent and IR-independent Phosphorylation of SMC3. *Journal of Biological Chemistry* **283**, 19176–19183 (2008).

59. E. Watrin, J.-M. Peters, The cohesin complex is required for the DNA damage-induced G2/M checkpoint in mammalian cells. *EMBO J* **28**, 2625–2635 (2009).

60. K. Choudhary, *et al.*, S. cerevisiae Cells Can Grow without the Pds5 Cohesin Subunit. *mBio* **13**, e01420-22 (2022).

61. G. Singh, R. V. Skibbens, Fdo1, Fkh1, Fkh2, and the Swi6-Mbp1 MBF complex regulate Mcd1 levels to impact eco1 rad61 cell growth in Saccharomyces cerevisiae. *Genetics* **228**, iyae128 (2024).

62. A. Toth, *et al.*, Yeast Cohesin complex requires a conserved protein, Eco1p(Ctf7), to establish cohesion between sister chromatids during DNA replication. *Genes & Development* **13**, 320–333 (1999).

63. L. M. D'Ambrosio, B. D. Lavoie, Pds5 Prevents the PolySUMO-Dependent Separation of Sister Chromatids. *Current Biology* **24**, 361–371 (2014).

64. R. Gandhi, P. J. Gillespie, T. Hirano, Human Wapl Is a Cohesin-Binding Protein that Promotes Sister-Chromatid Resolution in Mitotic Prophase. *Current Biology* **16**, 2406–2417 (2006).

65. S. Kueng, *et al.*, Wapl Controls the Dynamic Association of Cohesin with Chromatin. *Cell* **127**, 955–967 (2006).

66. B. D. Rowland, *et al.*, Building Sister Chromatid Cohesion: Smc3 Acetylation Counteracts an Antiestablishment Activity. *Molecular Cell* **33**, 763–774 (2009).

67. T. Sutani, T. Kawaguchi, R. Kanno, T. Itoh, K. Shirahige, Budding Yeast Wpl1(Rad61)-Pds5 Complex Counteracts Sister Chromatid Cohesion-Establishing Reaction. *Current Biology* **19**, 492–497 (2009).

68. S. Buskirk, R. V. Skibbens, G1-Cyclin2 (Cln2) promotes chromosome hypercondensation in *eco1/ctf7 rad61* null cells during hyperthermic stress in *Saccharomyces cerevisiae*. *G3 Genes|Genomes|Genetics* **12**, jkac157 (2022).

69. L. Lopez-Serra, A. Lengronne, V. Borges, G. Kelly, F. Uhlmann, Budding Yeast Wapl Controls Sister Chromatid Cohesion Maintenance and Chromosome Condensation. *Current Biology* **23**, 64–69 (2013).

70. M. E. Maradeo, R. V. Skibbens, The Elg1-RFC Clamp-Loading Complex Performs a Role in Sister Chromatid Cohesion. *PLoS ONE* **4**, e4707 (2009).

71. C. M. Zuilkoski, R. V. Skibbens, PCNA antagonizes cohesin-dependent roles in genomic stability. *PLoS ONE* **15**, e0235103 (2020).

72. K. Tong, R. V. Skibbens, Cohesin without Cohesion: A Novel Role for Pds5 in Saccharomyces cerevisiae. *PLoS ONE* **9**, e100470 (2014).

73. M. S. Bloom, D. Koshland, V. Guacci, Cohesin Function in Cohesion, Condensation, and DNA Repair Is Regulated by Wpl1p via a Common Mechanism in Saccharomyces cerevisiae. *Genetics* **208**, 111–124 (2018).

74. R. Ciosk, *et al.*, An ESP1/PDS1 Complex Regulates Loss of Sister Chromatid Cohesion at the Metaphase to Anaphase Transition in Yeast. *Cell* **93**, 1067–1076 (1998).

75. A. Yamamoto, Pds1p is required for faithful execution of anaphase in the yeast, Saccharomyces cerevisiae. *The Journal of Cell Biology* **133**, 85–97 (1996).

76. F. Uhlmann, F. Lottspeich, K. Nasmyth, Sister-chromatid separation at anaphase onset is promoted by cleavage of the cohesin subunit Scc1. *Nature* **400**, 37–42 (1999).

77. T. M. Leissing, L. M. Luh, P. M. Cromm, Structure driven compound optimization in targeted protein degradation. *Drug Discovery Today: Technologies* **37**, 73–82 (2020).

78. D. Khago, I. J. Fucci, R. A. Byrd, The Role of Conformational Dynamics in the Recognition and Regulation of Ubiquitination. *Molecules* **25**, 5933 (2020).

79. E. Blaszczak, *et al.*, Dissecting Ubiquitylation and DNA Damage Response Pathways in the Yeast Saccharomyces cerevisiae Using a Proteome-Wide Approach. *Mol Cell Proteomics* **23**, 100695 (2024).

80. D. L. Swaney, *et al.*, Global analysis of phosphorylation and ubiquitylation cross-talk in protein degradation. *Nat Methods* **10**, 676–682 (2013).

81. I. Litwin, *et al.*, ISW1a modulates cohesin distribution in centromeric and pericentromeric regions. *Nucleic Acids Research* **51**, 9101–9121 (2023).

82. X. Yang, *et al.*, The ubiquitin–proteasome system regulates meiotic chromosome organization. *Proc. Natl. Acad. Sci. U.S.A.* **119** (2022).

83. J. R. S. Newman, E. Wolf, P. S. Kim, A computationally directed screen identifying interacting coiled coils from *Saccharomyces cerevisiae*. *Proc. Natl. Acad. Sci. U.S.A.* **97**, 13203–13208 (2000).

84. M. Costanzo, *et al.*, A global genetic interaction network maps a wiring diagram of cellular function. *Science* **353** (2016).

85. W. Zhang, C. H. L. Yeung, L. Wu, K. W. Y. Yuen, E3 ubiquitin ligase Bre1 couples sister chromatid cohesion establishment to DNA replication in Saccharomyces cerevisiae. *eLife* **6**, e28231 (2017).

86. K. Tong, R. V. Skibbens, Pds5 regulators segregate cohesion and condensation pathways in *Saccharomyces cerevisiae*. *Proc. Natl. Acad. Sci. U.S.A.* **112**, 7021–7026 (2015).

87. M. L. Mayer, S. P. Gygi, R. Aebersold, P. Hieter, Identification of RFC(Ctf18p, Ctf8p, Dcc1p). *Molecular Cell* **7**, 959–970 (2001).

88. C. D'Ambrosio, G. Kelly, K. Shirahige, F. Uhlmann, Condensin-Dependent rDNA Decatenation Introduces a Temporal Pattern to Chromosome Segregation. *Current Biology* **18**, 1084–1089 (2008).

89. V. Guacci, E. Hogan, D. Koshland, Chromosome condensation and sister chromatid pairing in budding yeast. *The Journal of cell biology* **125**, 517–530 (1994).

90. T. Eng, V. Guacci, D. Koshland, Interallelic complementation provides functional evidence for cohesin–cohesin interactions on DNA. *MBoC* **26**, 4224–4235 (2015).

91. O. Orgil, *et al.*, A Conserved Domain in the Scc3 Subunit of Cohesin Mediates the Interaction with Both Mcd1 and the Cohesin Loader Complex. *PLoS Genet* **11**, e1005036 (2015).

92. J. Woodman, M. Hoffman, M. Dzieciatkowska, K. C. Hansen, P. C. Megee, Phosphorylation of the Scc2 cohesin deposition complex subunit regulates chromosome condensation through cohesin integrity. *Mol Biol Cell* **26**, 3754–3767 (2015).

93. V. Guacci, D. Koshland, Cohesin-independent segregation of sister chromatids in budding yeast. *MBoC* **23**, 729–739 (2012).

94. R. Ciosk, *et al.*, Cohesin's Binding to Chromosomes Depends on a Separate Complex Consisting of Scc2 and Scc4 Proteins. *Molecular Cell* **5**, 243–254 (2000).

95. M. E. Maradeo, R. V. Skibbens, Replication Factor C Complexes Play Unique Pro- and Anti-Establishment Roles in Sister Chromatid Cohesion. *PLoS ONE* **5**, e15381 (2010).

96. H. Yang, Q. Ren, Z. Zhang, Cleavage of Mcd1 by Caspase-like Protease Esp1 Promotes Apoptosis in Budding Yeast. *MBoC* **19**, 2127–2134 (2008).

97. Q. Ren, L.-C. Liou, Q. Gao, X. Bao, Z. Zhang, Bir1 Deletion Causes Malfunction of the Spindle Assembly Checkpoint and Apoptosis in Yeast. *Front. Oncol.* **2** (2012).

98. A. Varshavsky, The Ubiquitin System, Autophagy, and Regulated Protein Degradation. *Annu Rev Biochem* **86**, 123–128 (2017).

99. I. Livneh, Y. Kravtsova-Ivantsiv, O. Braten, Y. T. Kwon, A. Ciechanover, Monoubiquitination joins polyubiquitination as an esteemed proteasomal targeting signal. *Bioessays* **39** (2017).

100. F. Chen, *et al.*, Caspase Proteolysis of the Cohesin Component RAD21 Promotes Apoptosis. *Journal of Biological Chemistry* **277**, 16775–16781 (2002).

101. D. Pati, N. Zhang, S. E. Plon, Linking Sister Chromatid Cohesion and Apoptosis: Role of Rad21. *Molecular and Cellular Biology* **22**, 8267–8277 (2002).

102. J. M. Heidinger-Pauli, O. Mert, C. Davenport, V. Guacci, D. Koshland, Systematic reduction of cohesin differentially affects chromosome segregation, condensation, and DNA repair. *Curr Biol* **20**, 957–963 (2010).

103. M. D. Rose, F. Winston, P. Hieter, *Methods in yeast genetics* (Cold Spring Harbor Laboratory Press, 1990).

104. M. S. Longtine, *et al.*, Additional modules for versatile and economical PCR-based gene deletion and modification in Saccharomyces cerevisiae. *Yeast* **14**, 953–961 (1998).

105. M. A. Kenna, R. V. Skibbens, Mechanical Link between Cohesion Establishment and DNA Replication: Ctf7p/Eco1p, a Cohesion Establishment Factor, Associates with Three Different Replication Factor C Complexes. *Molecular and Cellular Biology* **23**, 2999–3007 (2003).

106. M. Foiani, F. Marini, D. Gamba, G. Lucchini, P. Plevani, The B Subunit of the DNA Polymerase α-Primase Complex in *Saccharomyces cerevisiae* Executes an Essential Function at the Initial Stage of DNA Replication. *Molecular and Cellular Biology* **14**, 923–933 (1994).

107. K. J. Livak, T. D. Schmittgen, Analysis of Relative Gene Expression Data Using Real-Time Quantitative PCR and the 2−ΔΔCT Method. *Methods* **25**, 402–408 (2001).

Figure Legends

Figure 1. Mcd1 protein levels are reduced in *eco1-203* and *rad61*Δ mutated cells. A) Flow cytometry data of DNA contents for wildtype (YPH499), *eco1-203* (YBS514), *rad61*Δ (YMM808) and *eco1*Δ *rad61*Δ (YBS829) mutant cells. Log phase cultures were synchronized in S phase at their respective permissive temperatures, 23°C for *eco1-203* and 30°C for wildtype *eco1*Δ *rad61*Δ and *rad61*Δ mutant cells, then shifted to 37°C for 1 hr. B) Representative Western Blot of Mcd1 (top panel) and Pgk1 (lower panel) protein obtained from extracts of HU-synchronized wildtype, *eco1-203*, *rad61*Δ and *eco1*Δ *rad61*Δ mutant cells indicated in (A). *

indicates non-specific band. C) Quantification of Mcd1, normalized to Pgk1 loading controls. Statistical analysis was performed using a two-tailed *t*-test. Statistical differences (*) are based on a $P < 0.05$ obtained across three experiments (n=3). Error bars indicate the standard deviation.

Figure 2. *MCD1* mRNA expression is increased in *eco1*Δ *rad61*Δ double mutant cells. A) Flow cytometry data of DNA content for log phase wildtype (YPH499) and *eco1*Δ *rad61*Δ (YBS829) double mutant cells arrested in S phase at 30°C for 3 hrs. B) Representative Western Blot of Mcd1 (top panel) and Pgk1 (lower panel) protein obtained from extracts of HU-synchronized wildtype and *eco1*Δ *rad61*Δ double mutant cells indicated in (A). C) Quantification of Mcd1, normalized to Pgk1 loading controls. Statistical analysis was performed using a two-tailed *t*-test. Statistical differences (**) are based on a $P < 0.01$ obtained across four experiments (n=4). Error bars indicate the standard deviation. D) Quantification of *MCD1* mRNA fold change normalized to the expression of the housekeeping gene *ALG9*. Statistical analysis was performed using a two-tailed *t*-test. Statistical differences (*) are based on a $P < 0.05$ obtained across four experiments (n=4). Error bars indicate the standard deviation.

Figure 3. Deletion of Ubiquitin E3 ligases *SAN1* and *DAS1* suppress the growth defects of *eco1*Δ *rad61*Δ double mutant cells. A) Growth of 10-fold serial dilutions of A) wildtype (YPH499), *bul2*Δ (YGS277), *eco1*Δ *rad61*Δ (YBS829) and two independent isolates of *eco1*Δ *rad61*Δ *bul2*Δ triple mutant cells (YGS279, YGS280); B) wildtype (YPH499), *bre1*Δ (YGS309), *eco1*Δ *rad61*Δ (YBS829) and two independent isolates of *eco1*Δ *rad61*Δ *bre1*Δ triple mutant cells (YGS292, YGS293); C) wildtype (YPH499), *lbd19*Δ (YGS281), *eco1*Δ *rad61*Δ (YBS829) and two independent isolates of *eco1*Δ *rad61*Δ *lbd19*Δ triple mutant cells (YGS282, YGS283); D) wildtype (YPH499), *san1*Δ (YGS284), *eco1*Δ *rad61*Δ (YBS829) and two independent isolates of *eco1*Δ *rad61*Δ *san1*Δ triple mutant cells (YGS286, YGS287); and E)

wildtype (YPH499), *das1*Δ (YGS288), *eco1*Δ *rad61*Δ (YBS829) and two independent isolates of *eco1*Δ *rad61*Δ *das1*Δ triple mutant cells (YGS290, YGS291). Temperature and days of growth are indicated.

Figure 4. Increased Mcd1 levels partially rescue the growth defects of cohesin mutated cells. A) Growth of 10-fold serial dilutions of cells (strains indicated below) that contains either 2μ vector (pRS424) or 2μ vector that contains *MCD1* (pBS1476). Two independent isolates are shown of mutated strains that express elevated levels of *MCD1*. Cell strains are as follows: A) wildtype (YGS209, YGS210) and *smc3-42* (YGS229, YGS230, YGS231); B) wildtype (YGS209, YGS210) and *smc1-259* (YGS211, YGS212, YGS213); C) wildtype (YBS4558, YBS4562) and *scc3-6* (YBS4568, YBS4569); D) wildtype (YGS209, YGS210) and *eco1-203* (YGS329, YGS330, YGS331); and E) wildtype (YGS216, YGS217) and *scc2-4* (YGS 218, YGS219, YGS220). Temperature and days of growth are indicated. Strain genotypes are provided in Supplementary Table 1.

Figure 5. Increased Mcd1 protein levels suppress *smc1-259* cell condensation defects. A) Flow cytometry data of DNA content for log phase cells pre-synchronized in G1 phase at 23°C, then shifted to 34°C (the non-permissive temperature of *smc1-259*) in nocodazole. Genotypes of wildtype (YGS335, YGS337) and *smc1-259* mutated (YGS338, YGS341) cells that contain either 2μ vector (pRS424) or 2μ vector that contains *MCD1* are provided in Supplementary Table 1. B) Representative micrographs of rDNA detected by Net1-GFP. DNA is detected by DAPI staining. C) The percentage of cells with condensed rDNA is plotted. At least 120 nuclei were scored per genotype. Statistical analysis was performed using a two-tailed *t*-test. Statistical differences (ns) are based on a $P > 0.05$ obtained across two experiments (n=2). Error bars indicate the standard deviation. D) The uncondensed rDNA structures for all strains were further classified as either fully decondensed “puffs” or partially

decondensed "partial". Statistical analysis was performed using a two-tailed *t*-test. Statistical differences (**) are based on a $P < 0.01$, and (***) are based on a $P < 0.001$ obtained across two experiments (n=2). Error bars indicate the standard deviation.

Figure 6 Increased Mcd1 levels in *smc1-259* cells significantly suppresses sister chromatid cohesion defects. A) Flow cytometry data of DNA content as described in Figure 5. B) Representative micrographs of GFP dots (markers of sister chromatid cohesion) in cell treatments as described in Figure 5. Genotypes of wildtype (YGS333, YGS334) and *smc1-259* mutated (YGS321, YGS323) cells modified to contain both cohesion cassettes and either 2μ vector (pRS424) or 2μ vector that contains *MCD1* are provided in Supplementary Table 1. C) The percentage of cells in which sisters are separated (two GFP spots indicated of a sister chromatid cohesion defect) is plotted. At least 120 cells were scored for each genotype. Statistical analysis was performed using a two-tailed *t*-test. Statistical differences (ns) are based on a $P > 0.05$, (*) are based on a $P < 0.05$ and (**) are based on a $P < 0.01$ obtained across two experiments (n=2). Error bars indicate the standard deviation.

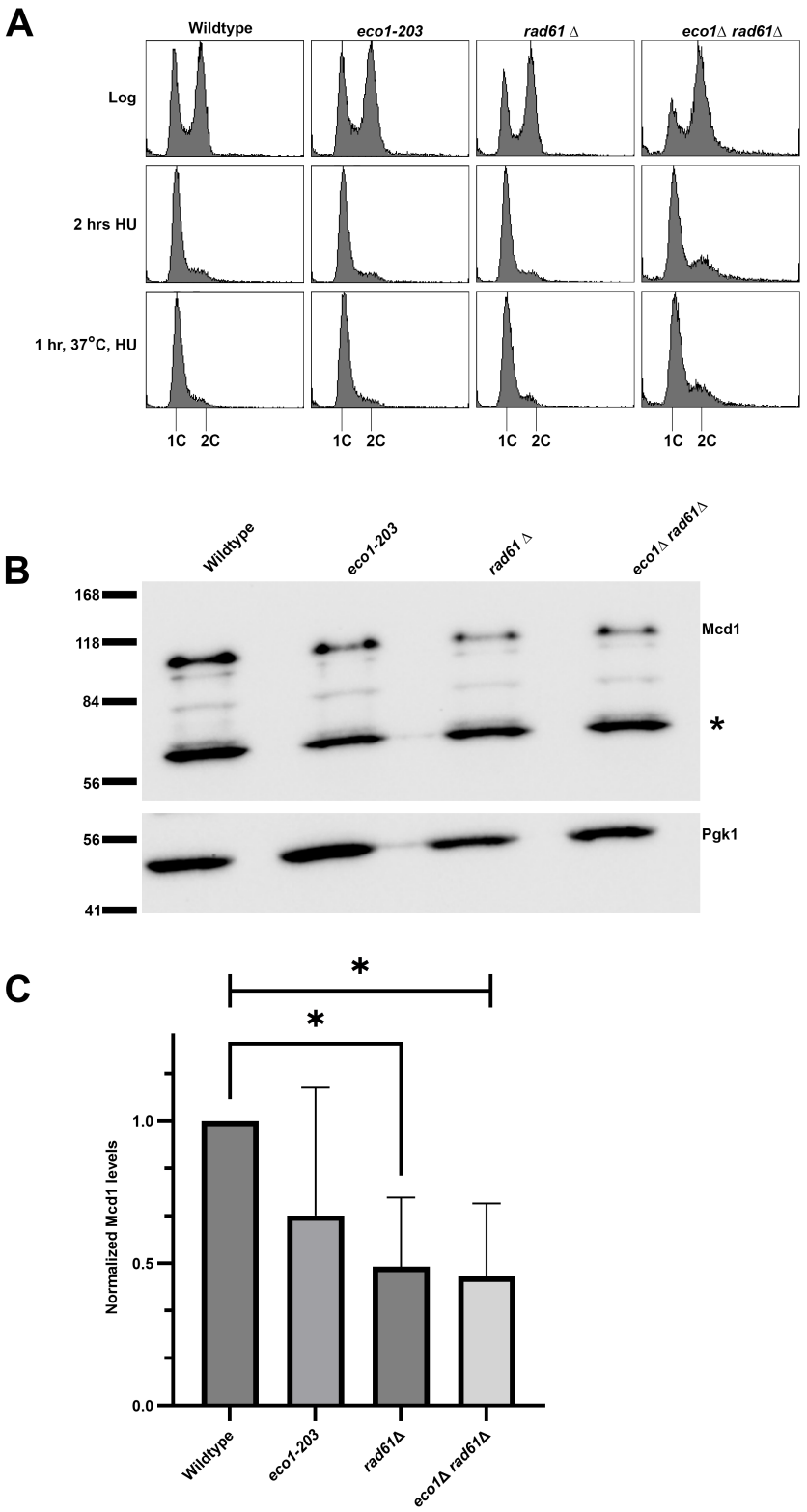

Figure 1

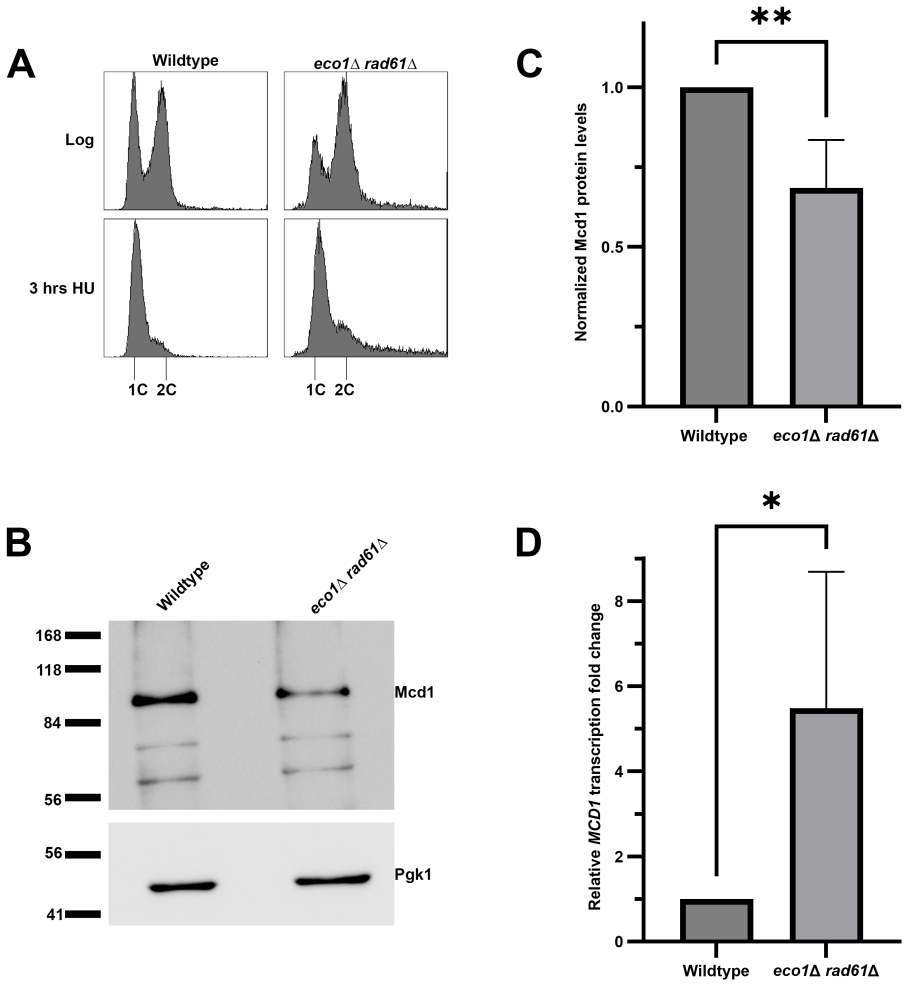

Figure 2

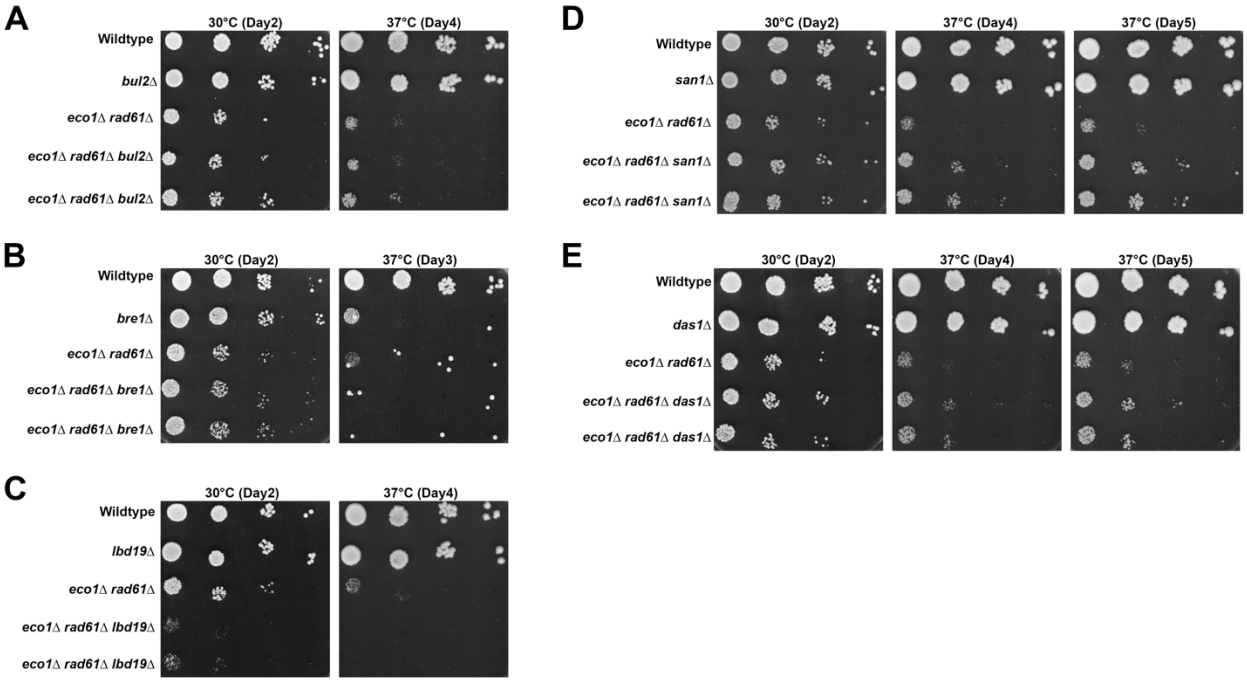

Figure 3

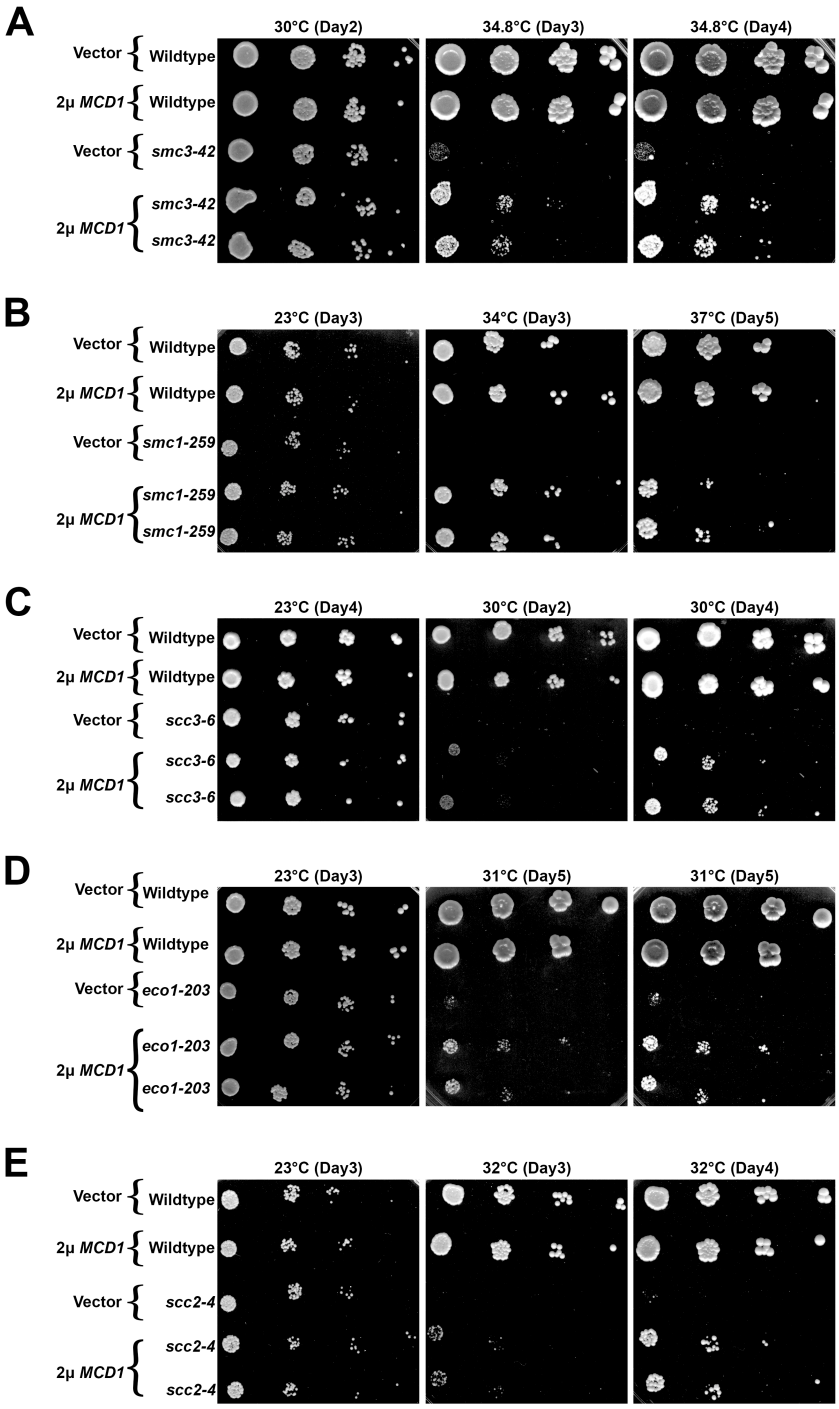

Figure 4

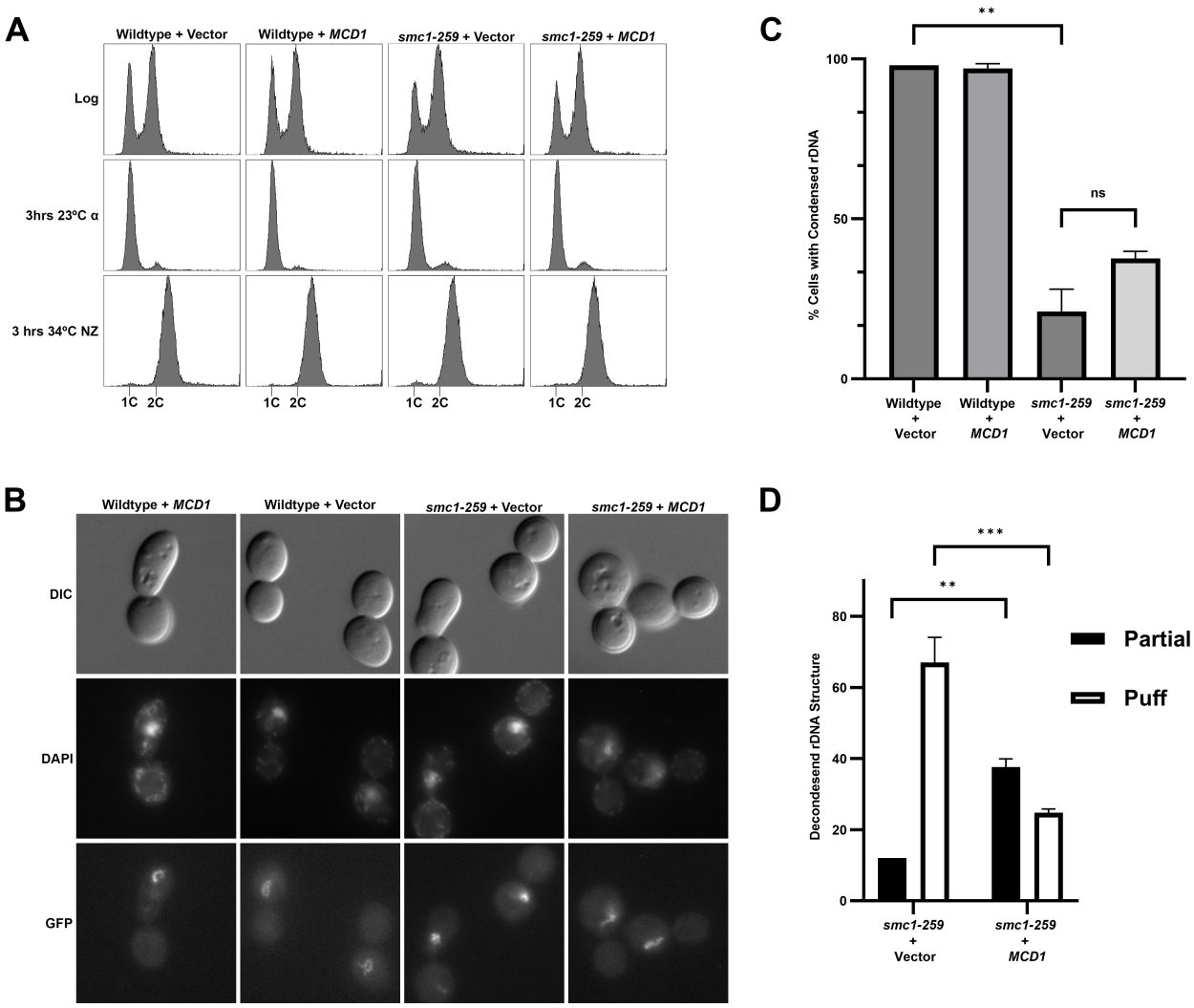

Figure 5

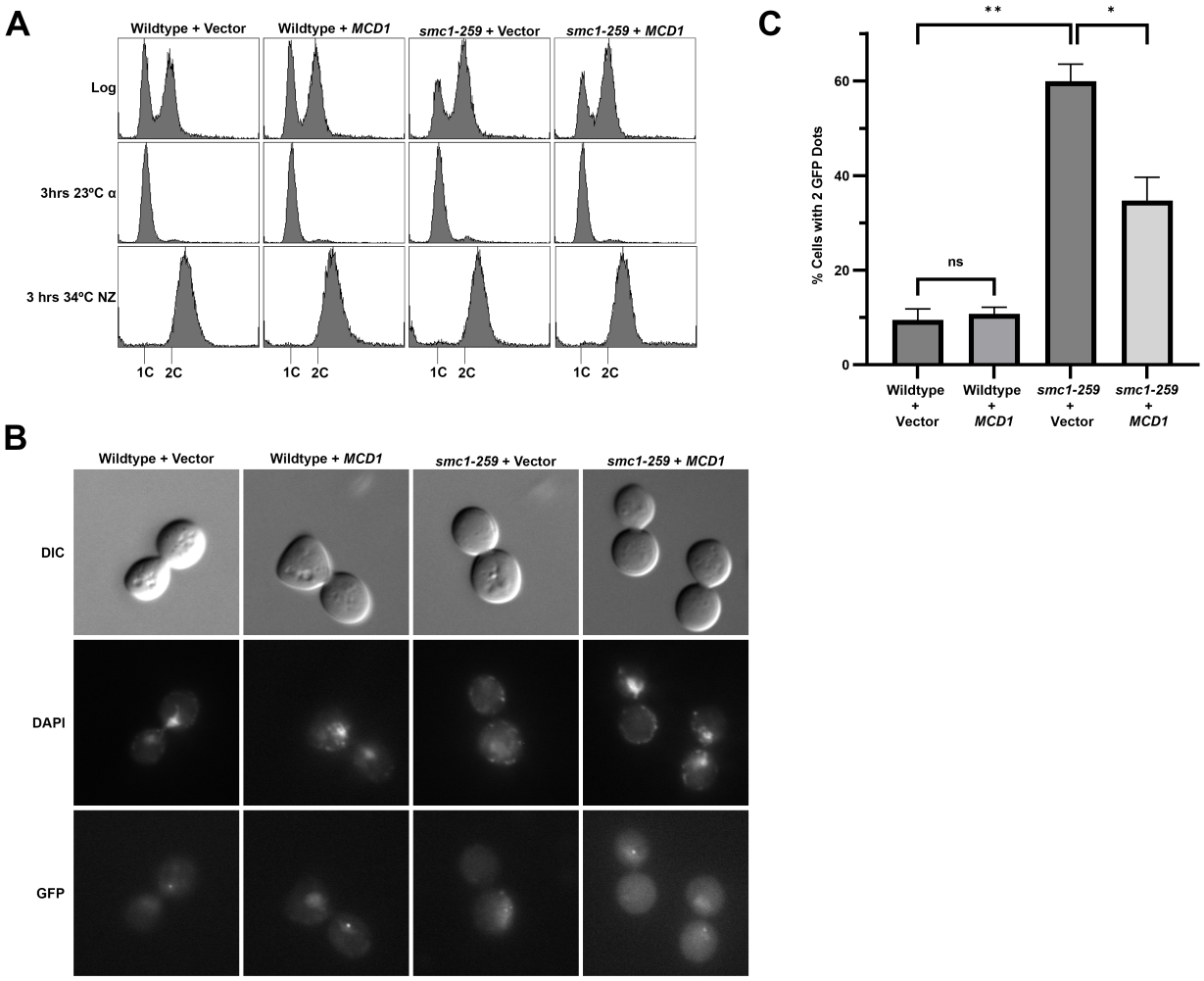

Figure 6